Chemical Science

EDGE ARTICLE

View Article Online
View Journal | View Issue

Cite this: *Chem. Sci.*, 2014, **5**, 4800

Near infra-red emitting Ru(II) complexes of tridentate ligands: electrochemical and photophysical consequences of a strong donor ligand with large bite angles†

Amlan K. Pal,[a] Scolastica Serroni,[b] Nelsi Zaccheroni,*[c] Sebastiano Campagna*[b] and Garry S. Hanan*[a]

A novel N^N^N tridentate ligand **dgpy** (**dgpy** = 2,6-diguanidylpyridine) was synthesized by a Pd-catalyzed C–N bond-forming reaction. A novel family of $[Ru^{II}(tpy')(\mathbf{dgpy})](PF_6)_2$ (**1** and **2**) or $[Ru^{II}(dpt')(\mathbf{dgpy})](PF_6)_2$ (**3** and **4**) (tpy' = substituted-2,2′:6′,2′-terpyridine, dpt' = substituted-2,4-dipyrid-2′-yl-1,3,5-triazine) complexes are reported. The **dgpy** ligand (80%) and the heteroleptic complexes **1–4** (37–60%) were obtained in modest to good yields. The **dgpy** ligand and its complexes were fully characterized by a variety of techniques including X-ray crystallography and density functional theory (DFT). In cyclic voltammetric studies, the complexes exhibit a $Ru^{III/II}$ couple, which is 600–800 mV less positive than the $Ru^{III/II}$ couple in $[Ru(tpy)_2]^{2+}$. The ^{1}MLCT absorption maxima of all the complexes (620–740 nm) are considerably red-shifted as compared to that of $[Ru(tpy)_2]^{2+}$ (474 nm). The ^{3}MLCT emission maxima of complexes **1** and **2** are also red-shifted by about 270 nm compared to that of $[Ru(tpy)_2]^{2+}$ (629 nm) at room temperature (298 K), whereas the corresponding maxima for complexes **3** and **4** are shifted by about 330 nm at 77 K. The relative trends in redox potentials and ^{1}MLCT maxima are in good agreement with DFT and TD-DFT calculations. Complexes **1** and **2** emit from a Ru^{II}-to-tpy ^{3}MLCT state, which is rarely the emitting state at $\lambda > 850$ nm in $[Ru(tpy)(N^N^N)]^{2+}$ complexes when the ancillary ligand is neutral. Complexes **1** and **2** also exhibit long excited-state lifetimes ($\tau \sim 100$ ns) at room temperature with associated quantum yield (Φ) of 0.001. The reported τ and Φ values are approximately 400–500 times and 1000 times higher compared to those of $[Ru(tpy)_2]^{2+}$ ($\tau = 0.25$ ns, $\Phi \leq 5 \times 10^{-6}$), respectively. Complexes **3** and **4** emit from a Ru^{II}-to-dpt ^{3}MLCT state, albeit only at 77 K ($\tau = 0.25$ ns) due to rapid deactivation of their ^{3}MLCT state according to the energy-gap law. The improved photophysical properties of the complexes are consequences of enlarged separation of the ^{3}MLCT–^{3}MC states, due to the strong donation and larger bite angles of the **dgpy** ligand.

Received 31st May 2014
Accepted 8th August 2014

DOI: 10.1039/c4sc01604a

www.rsc.org/chemicalscience

Introduction

Ru(II)-polypyridine complexes continue to draw considerable interest in the context of molecular electronics, photochemical conversion solar energy,[1] photoluminescence biosensors[2] and electroluminescent dyes in organic light-emitting devices[3] due to their remarkable redox and photophysical properties.[4–8] As effective light-harvesting materials, these compounds should exhibit (i) low energy metal-to-ligand charge transfer (MLCT) transitions, (ii) long room-temperature (r.t.) lifetimes of the excited ^{3}MLCT state, (iii) high emission quantum yields and (iv) a structural arrangement suitable to yield, upon synthetic elaboration, vectorial electron or energy transfer along a pre-designed direction.[9] Tris-bidentate Ru(II)-complexes, for example, $[Ru(bpy)_3]^{2+}$ (bpy = 2,2′-bipyridine) or its derivatives, are of particular interest in this context.[10] However, complexes of these types are often limited to tiresome stereoisomeric purification procedures, when they are incorporated into larger polynuclear assemblies and the desired vectorial transfer of electron or energy along a specific direction is not easily achieved.

In contrast to tris(bidentate)-Ru(II) complexes, achiral $[Ru(tpy)_2]^{2+}$ (tpy = 2,2′:6′,2′-terpyridine) type complexes are structurally more appealing due to their higher symmetry (D_{2d} instead of D_3 for $[Ru(bpy)_3]^{2+}$) and their inherent linearity and

[a]*Département de Chimie, Université de Montréal, Montréal, Québec, H3T 1J4, Canada. E-mail: garry.hanan@umontreal.ca*

[b]*Dipartimento di Scienze Chimiche, Università di Messina, Centro di ricerca interuniversitario per la conversione chimica dell'energia solare (SOLAR-CHEM), 98166 Messina, Italy*

[c]*Dipartimento di Chimica "G. Ciamician", Università di Bologna, 40126 Bologna, Italy*

† Electronic supplementary information (ESI) available. CCDC 978431 and 988217–988220. For ESI and crystallographic data in CIF or other electronic format see DOI: 10.1039/c4sc01604a

generation of isomerically pure rod-like multiunit assemblies when substituted along the C_2 axis.[6,11–16] Although the ground state properties of $[Ru(tpy)_2]^{2+}$ type complexes are similar to that of $[Ru(bpy)_3]^{2+}$ type complexes, the r.t. ^{3}MLCT excited-state lifetime of the former is limited to only 0.25 ns,[17a] nevertheless it has to be underlined that this does not prevent the successful incorporation of the former, or of its derivatives, into photovoltaic devices, such as dye-sensitized solar cells.[17b] This short lifetime in $[Ru(tpy)_2]^{2+}$ is due to rapid population and deactivation *via* short-lived and non-emissive triplet metal-centered (^{3}MC) state, which remains in close equilibrium with the emissive ^{3}MLCT state.[4,5a] The equilibrium has been attributed to the unfavourable bite angles of the *mer*-coordinated tridentate ligands, thereby generating a weak ligand field, leading to a low-lying thermally accessible ^{3}MC state, quasi iso-energetic to the ^{3}MLCT state.[18]

Much attention has been devoted to design and synthesis of new tpy based Ru(II)-complexes with extended excited-state lifetimes. The typical approach is to increase the energy gap between the ^{3}MLCT and ^{3}MC states (Fig. 1), which could be performed either by stabilizing the ^{3}MLCT state or destabilizing the ^{3}MC state or doing both at a time. Stabilization of ^{3}MLCT state can be achieved by substitution of the tpy ligand by electron-withdrawing substituents.[13,16,19] An alternative approach introduces coplanar aromatic moieties with extended π-conjugated systems to take advantage of increased delocalization in the acceptor ligand of the MLCT emitting state, thereby reducing the Franck–Condon factors for radiationless decay.[20–24] Another approach introduces an organic chromophore to establish an equilibrium between the ^{3}MLCT and the usually long-lived, organic chromophore triplet ^{3}LC (LC = ligand-centered) states, where the ^{3}LC state serves as an excited state storage element, leading to repopulation of the emissive ^{3}MLCT state.[15,25–28] All of these strategies have led to an increase in the r.t. lifetime of the excited ^{3}MLCT state, (τ = 1–200 ns, leaving aside the lifetimes attributed to the equilibrated state in the presence of organic chromophores, which can be significantly longer). However, in most cases, the 4′-position of the tpy ligand is already functionalized, which limits its use for further derivatization or nucleation in supramolecular assemblies.

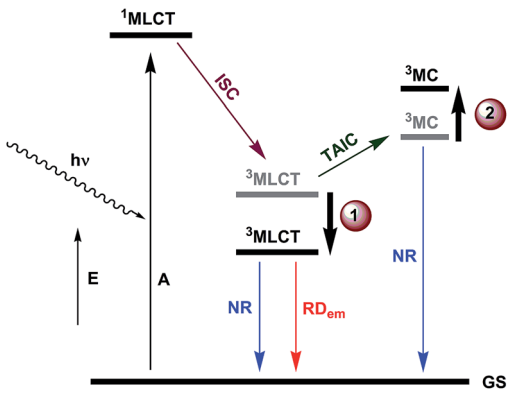

Fig. 1 Strategies to increase the emissive ^{3}MLCT lifetime of Ru(II)-polypyridyl complexes; (1) stabilizing the ^{3}MLCT state, (2) destabilizing the ^{3}MC state. (E = energy, A = absorption of photon, ISC = inter-system crossing, TAIC = thermally-activated internal conversion, NR = non-radiative decay, RD$_{em}$ = radiative decay).

As opposed to lowering the ^{3}MLCT state, an alternative method to increase the ^{3}MLCT–^{3}MC energy-gap is to raise the energy of the ^{3}MC state. This state can be destabilized by cyclometallating tridentate ligands (as N^C^N or N^N^C), which also red-shift the ^{3}MLCT excited state compared to N_6 analogues. Emission lifetimes in the range 4.5–106 ns has been reported with N^C^N type ligands.[10,29–35] Other types of strong σ-donor ligands, *e.g.*, N-heterocyclic carbenes (NHC), also give rise to relatively long r.t. excited-state lifetimes, for example ~8 μs in a heteroleptic Ru(II)-complex containing a substituted tpy.[35b] The ^{3}MC state can also be destabilized by increasing the ligand field strength by widening the ligand bite angle, thus making the coordination geometry around the metal-ion more octahedral. Following this approach, the introduction of alkyl (–CRR′–, where R = Me, R′ = OH, OMe) spacer in BPy-Py ligands or –CO– spacer in polypyridyl systems, increases the lifetime to 1.4 ns to 3.3 μs (in deareated solutions), respectively,[36–39] whereas Ru(II)-homoleptic complexes containing **dqp** (**dqp** = 2,6-di(quinoline) pyridine) ligand, exhibit long excited-state lifetimes (τ = 5.5 μs) and high quantum yields (Φ = 0.07).[40] It has been shown that the concept of introduction of wider bite angle of tridentate ligands not only helps to increase the r.t. excited-state lifetime, but also the quantum yield of the resulting complexes.[36b,40] The combination of ideal octahedral geometry using **dqp** ligand and an equilibrated ^{3}LC state with phenyl-anthracene, has also lead to a homoleptic Ru(II) complex that exhibits the longest r.t. excited-state lifetime (τ = 42 μs) reported so far.[28b]

We recently reported a series of tris-bidentate Ru(II) complexes, where a bpy unit had been substituted by a guanidyl-N-heterocyclic moiety. The introduction of an electron-rich guanidine unit significantly red-shifted the ^{1}MLCT and ^{3}MLCT states for these complexes as compared to $[Ru(bpy)_3]^{2+}$ (440 nm/620 nm) due to decreased chelate ring strain and strong donation.[41] To this end, we prepared a novel symmetrical tridentate ligand (**L1**) by coupling two of **H-hpp** units (**H-hpp** = 1,3,4,6,7,8-hexahydro-2*H*-pyrimido[1,2-(*a*)]pyrimidine) with 2,6-dibromopyridine. The **H-hpp** as the coupling agent can be introduced by C–N coupling in good yield.[42,43] The aliphatic backbones on **hpp** increases the strong σ-donor character of **L1** as compared to tpy. The chelating nitrogen atoms in the ligand form two 6-membered chelate rings with the central pyridine ring, thereby offering larger bite angles upon coordination to Ru(II) with near-octahedral geometry.[37,44,45] The last two modifications destabilize the ^{3}MC state, as discussed earlier.

Herein, we present the synthesis and characterization of novel heteroleptic Ru(II) complexes containing substituted tpy (**1–2**) ligands and substituted 2,4-dipyrid-2′-yl-triazine (dpt) ligands (**3–4**) together with **dgpy** (**L1**). Furthermore, the choice tpy and dpt was to examine the effect of planarity in triazine-related complexes compared to that of tpy-based compounds.[21,22] Due to the introduction of the triazine core, which remains in-plane with its peripheral aryl moieties, the ^{3}MLCT state is more stabilized and this is expected to induce

longer excited-state lifetime and also further red-shift compared to those exhibited by the tpy analogues. The redox and photophysical consequences due the strong donor **hpp** units are also reported.

Results and discussion

Syntheses of the ligands

The N-heterocyclic-guanidyl ligand, **L1** (2,6-diguanidylpyridine or **dgpy**) (Scheme 1) was synthesized by reaction of **H-hpp** with 2,6-dibromopyridine by Pd-catalyzed C–N bond forming reaction[46] following a recently published procedure.[41d] In the ligand **L1**, incorporation of a heterocycle at the amidine N*H* position of **H-hpp** renders the six annular methylene units chemically nonequivalent by NMR spectroscopy in contrast to the free **H-hpp** where only three types of methylene groups exist. A similar observation was reported by Coles and co-workers for a methylene-linked bis(guanidine) compound, $H_2C\{hpp\}_2$.[47]

The ligand 2,4-dipyrid-2′-yl-6-(*p-tert*-butylphenyl)-1,3,5-triazine (**L2**) was synthesized using a modified literature procedure (Scheme 1).[48] The amidinate intermediate generated by the reaction of "*in situ*" synthesized $LiNMe_2$ (from $HNMe_2$ and *n*-BuLi) and *p-tert*-butylbenzonitrile, could be subsequently cyclized by addition of 2 equivalents of 2-cyanopyridine to afford **L2** as a white solid in good yield (65%).

Syntheses of the complexes

Ru(II)-heteroleptic complexes were synthesized following the typical procedure available for the synthesis of bis-terpyridyl based Ru(II)-complexes (Scheme 2).[49] The reaction of **L1** with [Ru(Ph-tpy)Cl_3] (Ph-tpy = 4′-phenyl-2,2′:6′,2″-terpyridine), [Ru(*p*-Tolyl-tpy)Cl_3] (*p*-Tolyl-tpy = 4′-tolyl-2,2′:6′,2″-terpyridine), [Ru(Br-Ph-dpt)Cl_3] (Br-Ph-dpt = 2,4-dipyrid-2′-yl-6-(*p*-bromophenyl)-1,3,5-triazine), or [Ru(^{t}Bu-Ph-dpt)Cl_3] (^{t}Bu-Ph-dpt = 2,4-dipyrid-2′-yl-6-(*p-tert*-butyl-phenyl)-1,3,5-triazine) in refluxing *n*-butanol in presence of few drops of 4-ethylmorpholine provided the complexes **1**, **2**, **3** and **4**, respectively, in modest to good yields (37–60%).

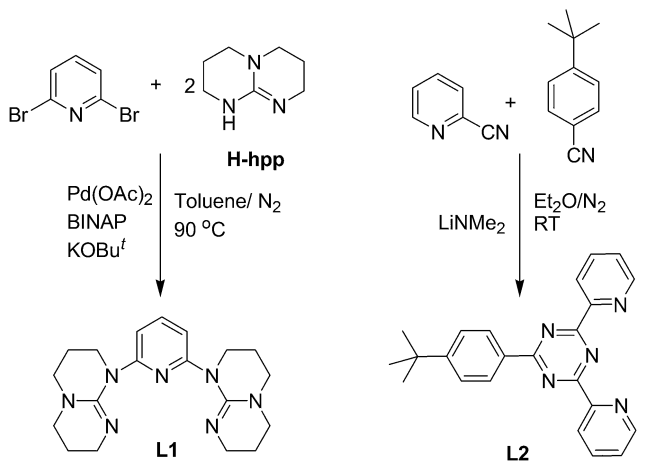

Scheme 1 Syntheses of the ligands L1 and L2.

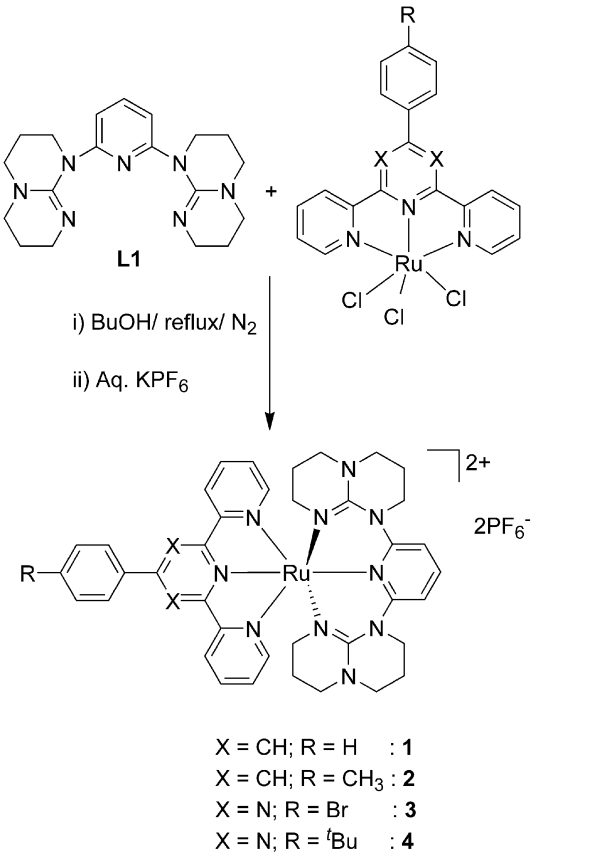

Scheme 2 Syntheses of the terpyridine (tpy, **1–2**) and 2,4-dipyrid-2′-yl-triazine (dpt, **3–4**) containing complexes.

The ligands **L1** and **L2** and complexes **1–4** were characterized by solution NMR spectroscopy, elemental analysis, X-ray crystallography and high-resolution mass spectrometry (HR-MS), UV-vis absorption and emission spectroscopies and electrochemistry. In HR-MS, the most abundant peaks were found to be $[M + H]^+$ and $[M]^{2+}$ for ligands and complexes, respectively.

Multiple unidentified colored byproducts, as also observed by Hammarström *et al.*,[44] were always found to be formed, and thus the complexes were purified by column chromatography followed by recrystallization from acetone solutions of **1–4** as purple solids.

In solution NMR spectroscopy, the most interesting feature in the ^{1}H NMR spectra of **1–4** is that the equatorial and axial methylene protons on the saturated aliphatic backbone are different, so that they appear over a wide range of 0–4 ppm integrating to two protons each. They are chemically nonequivalent to the methylene protons of **L1**, where only six different methylene proton signals were observed, each integrating for four protons.[41]

X-ray diffraction studies

Slow diffusion of diethyl ether into an acetone solution of **1–4** afforded the best single crystals, whereas crystals of **L1** could be grown by slow evaporation of a solution containing **L1** in diethyl ether. Some crystal parameters are included in Table 1.

Ligand **L1** and complexes **1**, **3** and **4** crystallize in monoclinic crystal system, whereas complex **2** crystallizes in triclinic system. The optimized ground state geometries of **1–4** are in reasonable agreement with the structural data (Table S1 and Fig. S2 in ESI†). The structure of ligand **L1** (Fig. 2) reveals that the guanidine moieties adopt more stable twisted chair conformations instead of higher energy boat conformation. To minimize the lone pair-lone pair repulsions, atoms N1, N4 and N7 adopt *trans* geometry around their respective C–N bonds. The N2–C12 [1.409(3) Å] and N3–C12 [1.383(3) Å] bond distances may suggest that there is delocalization around N2–C12–N3 core, whereas, N4–C12 seems to be a localized C–N double bond with a distance of 1.278(3) Å. Similar variation in bond lengths were also observed in the other saturated part of **L1** [N5–C19 (1.409(3) Å), N6–C19 (1.388(3) Å), N7–C19 (1.260(3) Å)]. Extensive non-aromatic weak C–H hydrogen bonding interactions among the saturated aliphatic backbone play an important role in the solid-state packing of molecule **L1** to furnish a 2D- zigzag array (see Fig. S1 in ESI†).

The structures of **1–4** (Fig. 3–6) reveal coordinatively saturated ruthenium atoms in a distorted octahedral geometry, where the two tridentate ligands coordinate in a meridional fashion, which is also supported by DFT calculations. Selected bond lengths and angles are in good agreement with the values obtained from DFT calculations of respective complexes (Table S1 in ESI†). The origin of distortion from regular octahedron in these complexes is due to the smaller bite angles subtended to the metal center by the two tridentate ligands. The trans N–Ru–N angles generated by Ph-tpy [159.28(10)°] and Tolyl-tpy [158.89(8)°] in complexes **1** and **2** are similar to the observed average bite angles in homoleptic $[Ru(Ph\text{-}tpy)_2]^{2+}$ [158.07(15)°][50]

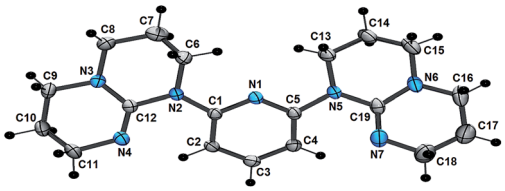

Fig. 2 Perspective view of ligand **L1**. Thermal ellipsoids are shown at a 50% probability level.

and $[Ru(Tolyl\text{-}tpy)_2]^{2+}$ [157.49(16)°],[51] respectively. The ligand **L1** exhibits trans N–Ru–N angles near ~173° [N4–Ru1–N10 = 173.83(10)° and 172.68(7)° in **1** and **2**, respectively], which are very close to ideal octahedral angle of 180°. This is a significant improvement over the non-ideal value of 158.2°, exhibited by tpy in prototype[52] $[Ru(tpy)_2]^{2+}$, suggesting a successful design strategy. Both complexes display regular Ru–N bond distances, the shortest Ru–N bonds consisting the N-atom of the central pyridyl unit in tpy core [Ru1–N2 = 1.946(2) Å and 1.931(2) Å in **1** and **2**, respectively], while the longest are the coordinate bonds from the **hpp** units [Ru1–N10 = 2.092(3) Å and Ru1–N4 = 2.095(2) Å in **1** and **2**, respectively]. In both the complexes, a twisted structure of ligand **L1** is observed, where the dihedral angles between the mean plane containing central pyridine ring and that of **hpp** units are in an average 43° (in **1**) and 35° (in **2**), which twist **L1** into a helical arrangement (Λ or Δ) around the Ru-atom. As opposed to other coordination complexes incorporating (CH_2)-bridged donor atoms,[53] the conformation of the saturated rings do not appear to have any noticeable influence on the Ru(II) structures.

Table 1 Crystalllographic data of ligand **L1** and complexes **1**·[6(C_3H_6O)], **2**·[C_3H_6O], **3**·[C_3H_6O], **4**·[8(C_3H_6O)]·[H_2O]

Compound	**L1**	**1**·[6(C_3H_6O)]	**2**·[C_3H_6O]	**3**·[C_3H_6O]	**4**·[8(C_3H_6O)]·[H_2O]
CCDC number	988217	978431	988218	988219	988220
Formula	$C_{19}H_{27}N_7$	$[C_{40}H_{42}N_{10}Ru]$ $[PF_6]_2\cdot[6(C_3H_6O)]$	$[C_{41}H_{44}N_{10}Ru]$ $[PF_6]_2\cdot[C_3H_6O]$	$[C_{38}H_{39}N_{12}BrRu]$ $[PF_6]_2\cdot[C_3H_6O]$	$[C_{42}H_{48}N_{12}Ru]$ $[PF_6]_2\cdot[8(C_3H_6O)]\cdot[H_2O]$
M_w (g mol^{-1}); d_{calcd} (g cm^{-3})	353.48; 1.307	1053.83; 2.164	1125.95; 1.622	1134.69; 1.713	1111.93; 1.354
T (K); F(000)	200; 1520	100; 6224	150; 1148	100; 2400	150; 2264
Crystal system	Monoclinic	Monoclinic	Triclinic	Monoclinic	Monoclinic
Space group	$C2/c$	$C2/c$	$P\bar{1}$	$P2(1)/n$	$P2(1)/c$
Unit cell					
a (Å)	16.6894(3)	40.9186(5)	8.5139(2)	8.5505(3)	9.6046(4)
b (Å)	13.1912(2)	12.9990(2)	13.5117(4)	44.2040(14)	32.8531(14)
c (Å)	17.1396(3)	19.2466(2)	21.1951(6)	12.3222(4)	17.3497(8)
α (°)	90	90	96.6310(10)	90	90
β (°)	107.7520(10)	116.1840(10)	94.8820(10)	96.705(2)	94.903(2)
γ (°)	90	90	106.4660(10)	90	90
V (Å^3); Z	3593.67(11); 8	9186.7(2); 8	2304.75(11); 2	4625.5(3); 4	5454.5(4); 4
θ range (°); completeness	4.36–72.14; 0.978	2.41–70.71; 0.996	5.46–69.31; 0.988	3.75–71.17; 0.994	3.71–69.36; 0.995
R_{fle}: collec./indi-pendent; R_{int}	17 487/3481; 0.0390	177 747/8737; 0.0265	69 864/8487; 0.0374	62 112/7553; 0.1031	217 905/9987; 0.0425
μ (mm^{-1})	0.654	4.637	4.275	5.286	3.602
$R_1(F)$; w$R(F^2)$; GoF(F^2)[a]	0.0727; 0.2055; 1.046	0.0468; 0.1299; 1.038	0.0345; 0.0950; 1.039	0.0457; 0.1239; 1.036	0.0402; 0.1129; 1.045
Residual electron density	1.304; −0.392	1.914; −0.777	0.713; −0.818	1.220; −0.664	0.763; −0.776

[a] $R_1(F)$ based on observed reflections with $I > 2\sigma(I)$ for **L1** and the complexes; w$R(F^2)$ and GoF(F^2) based on all data for all compounds.

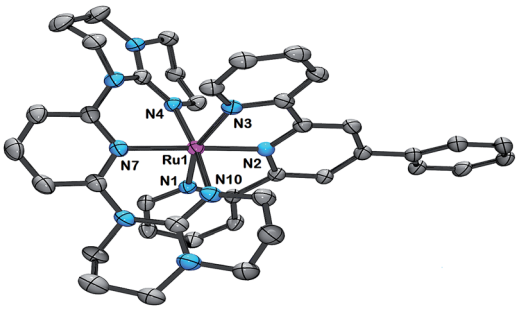

Fig. 3 Perspective view of complex **1**, with partial labeling. Hydrogen atoms and PF_6 anions are omitted for clarity. Thermal ellipsoids are shown at a 50% probability level.

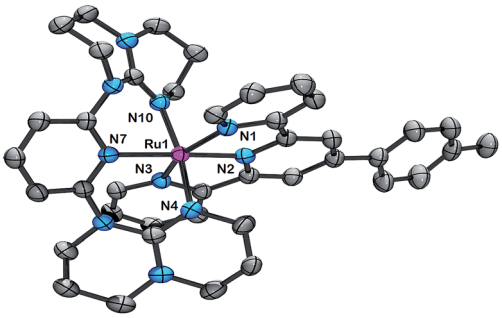

Fig. 4 Perspective view of complex **2**, with partial labeling. Hydrogen atoms, solvated acetone molecule and PF_6 anions are omitted for clarity. Thermal ellipsoids are shown at a 50% probability level. One disordered part in the aliphatic backbone has been omitted for clarity.

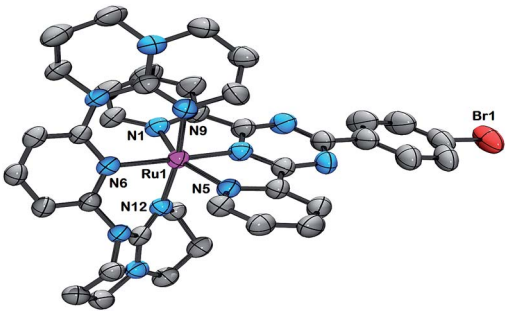

Fig. 5 Perspective view of complex **3**. Hydrogen atoms, solvated acetone molecule and PF_6 anions are omitted for clarity. Thermal ellipsoids are shown at a 50% probability level.

Complexes **3** and **4** are essentially isostructural with **1** and **2**. The shortest Ru–N bonds consisting the nitrogen of the central triazine unit [Ru1–N2 = 1.925(3) Å in **3** and 1.930(2) Å in **4**]. The N1–Ru1–N5 angles of the dpt unit [= 157.11(11)° in **3** and 156.29(9)° in **4**] are similar to what is found in dpt–Ru–dpt homoleptic complexes [N–Ru–N = 155.45(19)°].[54] Similarly to complexes **1** and **2**, N–Ru–N angles of **L1** in **3** and **4** expand up to ~172° [N9–Ru1–N12 = 172.14(11)° in **3** and N6–Ru1–N12 = 171.02(8)° in **4**], which should help to increase their ligand field effects and, therefore, the ^{3}MLCT–^{3}MC energy-gap.

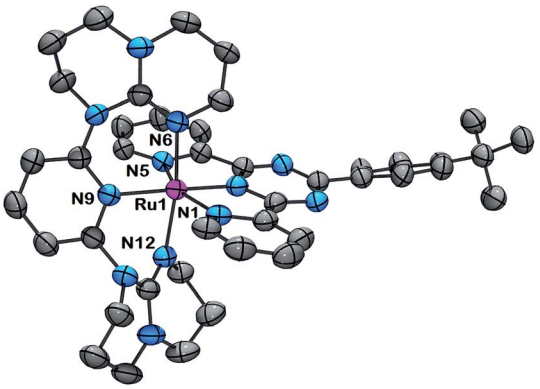

Fig. 6 Perspective view of complex **4**. Hydrogen atoms and PF_6 anions are omitted for clarity. Thermal ellipsoids are shown at a 50% probability level. One disordered part in the aliphatic backbone has been omitted for clarity.

Electrochemistry

The electrochemical behavior of the complexes has been examined by cyclic voltammetry using a glassy carbon electrode in purified acetonitrile under a dry argon atmosphere. At positive potentials, *vs.* saturated calomel electrode (SCE), complex **1** shows a quasi-reversible Ru(III/II) couple at 0.50 V with a peak to peak separation (ΔE_p) of 95 mV (Table 2). This is nearly 0.80 V less positive than that observed for the same Ru(III/II) couple in $[Ru(tpy)_2]^{2+}$ which appears at 1.31 V *vs.* SCE,[55] indicating that **L1** is a much stronger donor than tpy. Complex **2** shows a quasi-reversible Ru(III/II) couple at even lower potential, 0.46 V *vs.* SCE. The lowering by 40 mV in the corresponding oxidation potentials between complex **1** and **2** is due to minor destabilization of the metal-based highest-occupied molecular orbital (HOMO) by more electron-donating *p*-Tolyl-tpy in place of Ph-tpy, which is supported by DFT calculations (E_{HOMO} = −5.37 eV and −5.34 eV in **1** and **2**, respectively) (see Fig. 7 for population analyses). The Ru(III/II) couples for **1** and **2** are more similar to the values obtained for the cyclometallated complex [Ru(tpy)(1,3-di(2-pyridyl)benzene)]$^+$ and its derivatives.[56,57] The Ru(III/II) couple for [Ru(tpy)(1,3-di(2-pyridyl)benzene)]$^+$ appears at 0.51 V *vs.* SCE,[56] which indicates that the donor capacity of **L1** is similar to that of a cyclometallating anionic ligand. At negative potentials, complexes **1** and **2** display two quasi-reversible ligand-based reduction peaks (Fig. 8). The more electron-rich metal center in **1** and **2** compared to that of $[Ru(tpy)_2]^{2+}$ increases back-donation to both ligands and accordingly shifts the ligand-based reduction to more negative potentials, albeit to a lesser extent than observed for the oxidation couple. Such observations were previously reported by several groups.[42,56] The first reduction peak for complex **1** is centered at −1.47 V while that for complex **2** is at −1.52 V. Both these reduction peaks are tpy-based, which is also suggested by their respective DFT calculations in which a minor destabilization of the tpy-based lowest unoccupied molecular orbital (LUMO) of **1** (E_{LUMO} = −2.46 eV) compared to that of **2** (E_{LUMO} = −2.45 eV) is found. The second reduction peak for **1** had a potential of −2.01 V whereas that for **2** is centred at −2.05 V. The LUMO+1 for both the complexes are

Table 2 Half-wave potentials for Ru(II) complexes **1–4** and some benchmark complexes

Cmpd	$E_{1/2}$(ox)[a]	$E_{1/2}$(red)[a]	$\Delta E_{1/2}$[b]
L1	1.11 (308), 0.77 (irr)[c]	—	—
1	0.50 (94)	−1.47 (70), −2.01 (84)	1.97
2	0.46 (95)	−1.52 (77), −2.05 (83)	1.98
3	0.71 (82)	−0.92 (72), −1.72 (irr)[c]	1.63
4	0.67 (85)	−0.97 (63), −1.70 (90)	1.64
$[Ru(tpy)_2]^{2+}$	1.31 (60)[d]	−1.23 (70)[d], −1.47 (69)[d]	2.54
$[Ru(p\text{-Tolyl-tpy})_2]^{2+}$	1.20 (69)[e]	−1.29 (66)[e], −1.53 (74)[e]	2.49
$[Ru(Ph\text{-tpy})_2]^{2+}$	1.29[f]	−1.26[f]	2.55
[Ru(tpy)(N^C^N)]$^+$	0.51[g]	−1.55[g]	2.06
[Ru(tpy)(Br-Ph-dpt)]$^{2+}$	1.43[h]	−0.75[h]	2.18

[a] Potentials are in volts *vs.* SCE for acetonitrile solutions, 0.1 M in tetrabutylammonium hexafluorophosphate, under a dry argon atmosphere at a glassy carbon electrode, recorded at 25 ± 1 °C at a sweep rate of 100 mV s^{-1} with solute concentrations of **1** and **2**, 1.01 mM; **3**, 1.03 mM; **4**, 1.02 mM. The difference between cathodic and anodic peak potentials (millivolts) is given in parentheses. [b] Difference between the first oxidation and first reduction potentials (volt). [c] Irreversible; potential is given for the anodic wave. [d] From ref. 55*a*. [e] From ref. 55*c*. [f] From ref. 16*a*. [g] From ref. 56. [h] From ref. 54.

located principally on the respective tpy units. Thus, in a very coarse approximation, the second quasi-reversible reductions in **1** and **2** may also be assigned to tpy-based reductions, especially when no ligand-based reduction is observed in free **L1** within a potential range of 0 to −2 V, although more detailed calculations are necessary to confirm this assignment.

The electrochemical studies of the 2,4-dipyrid-2′-yl-triazine (dpt) complexes **3** and **4** also show similar trends. The Ru(III/II) couple appears at 0.71 and 0.67 V *vs.* SCE for **3** and **4**, respectively. These more positive values as compared to **1** and **2** are due to the replacement of the terpyridines with more π-accepting triazines, which reduces the electron density at the metal center. It is noteworthy that the Ru(III/II) couples for **3** and **4** are more than 0.7 V less positive than the corresponding couple in tpy–Ru–dpt heteroleptic complexes.[54] The back π-donation effect is also evident in case of **3** and **4**. The first reduction of **3**, which is triazine based, appears at −0.92 V, while it is observed at −0.97 V *vs.* SCE for **4**. These values are nearly 0.2 V more negative than the corresponding tpy–Ru–dpt heteroleptic complexes (Table 2).[54]

The above results clearly indicate that **L1** is a stronger donor than the classical polypyridine tridentate ligands. The donor ability is also comparable to cyclometallating ligands, a property which is very beneficial to destabilize the ^{3}MC state.

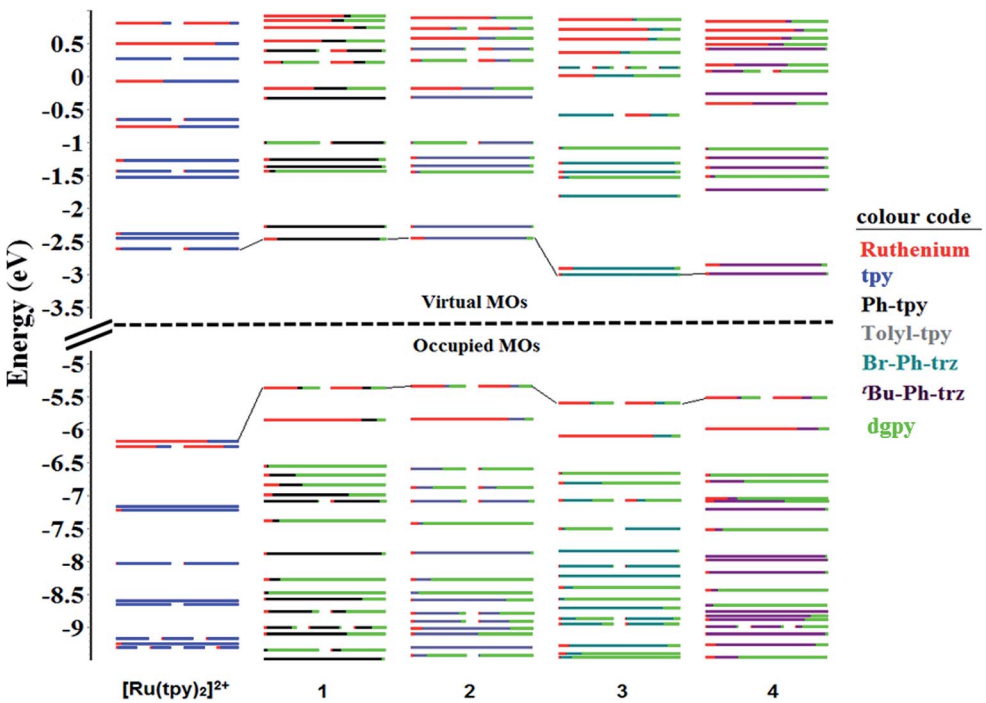

Fig. 7 Calculated frontier MO energies of the modeled **1–4** with $[Ru(tpy)_2]^{2+}$ obtained by DFT(RB3LYP)/LanL2DZ(f)[Ru]6-31G**[NCN] calculation with CPCM(CH_3CN) and 0.05 eV of threshold of degeneracy.

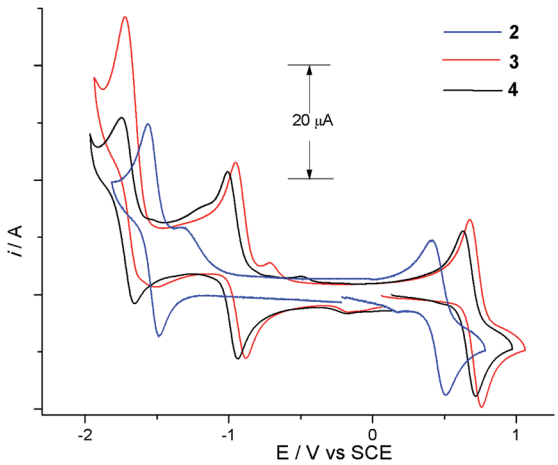

Fig. 8 Cyclic voltammograms of the complexes **2** (blue), **3** (red) and **4** (black) in dry, degassed acetonitrile.

UV-vis absorption and emission behavior

The UV-vis spectra of **1** and **2** in acetonitrile solution display the ^{1}MLCT bands in the 500–650 nm regions. The UV part of the spectra is dominated by the $\pi \rightarrow \pi^*$ transitions in the ligand moieties centered around 220–320 nm for both **1** and **2** (Fig. 9 and Table S2 in ESI†). The most noticeable feature in the visible region is that the ^{1}MLCT maxima is red-shifted (148 nm) with respect to that of $[Ru(tpy)_2]^{2+}$ for both complexes.[58] As discussed above, ligand **L1** being a stronger donor than tpy, is expected to interact with the t_2 [d(Ru)] orbitals of ruthenium more strongly than does tpy. Thus the metal based t_2 orbitals will be at higher energy, *i.e.* the HOMO will be raised. A minor, but noticeable, change due to the change in tpy backbone from phenyl (in **1**) to the more electron-donating tolyl group (in **2**) can also be observed, as supported by DFT calculations (Fig. 7 and Tables S3 and S5 in ESI†). On the other hand, the LUMO is still tpy-based as revealed by the first reduction potentials of **1** and **2** and DFT calculations. This fact results in lowering of the energy of the $d\pi \rightarrow \pi^*$ ^{1}MLCT transition and hence the observed red shift. Moreover, the complexes exhibit an additional band at approximately 380 nm between the ^{1}MLCT transition and the first $\pi \rightarrow \pi^*$ transition. Its assignment, though discussed in the literature, is still controversial, and different authors have proposed a metal centered d–d transition,[59] which borrows intensity from a close-lying allowed transition or to a second ^{1}MLCT or to ^{1}LMCT transition.[60] However, TD-DFT calculations of the complexes suggest that this band is a mixture, predominantly of ^{1}MLCT origin with minor involvement of a LC transition (see Tables S4 and S6 in ESI†).[41] It may be noted that such a band near 345 nm is usually observed for $[RuN_4(diamine)]^{2+}$ chromophores.[61]

Complexes **3** and **4** also exhibit similar ligand $\pi \rightarrow \pi^*$ transitions in the UV region centered on 244 and 290 nm for both the complexes. In the visible region both **3** and **4** absorb in the 500–800 nm region with maxima around 560 nm and 740 nm. This is a notable red-shift with respect to tpy-Ru–dpt heteroleptic complexes (264 nm) or even homoleptic dpt–Ru–dpt complexes (250 nm).[54] Such a red-shift is in accordance with the

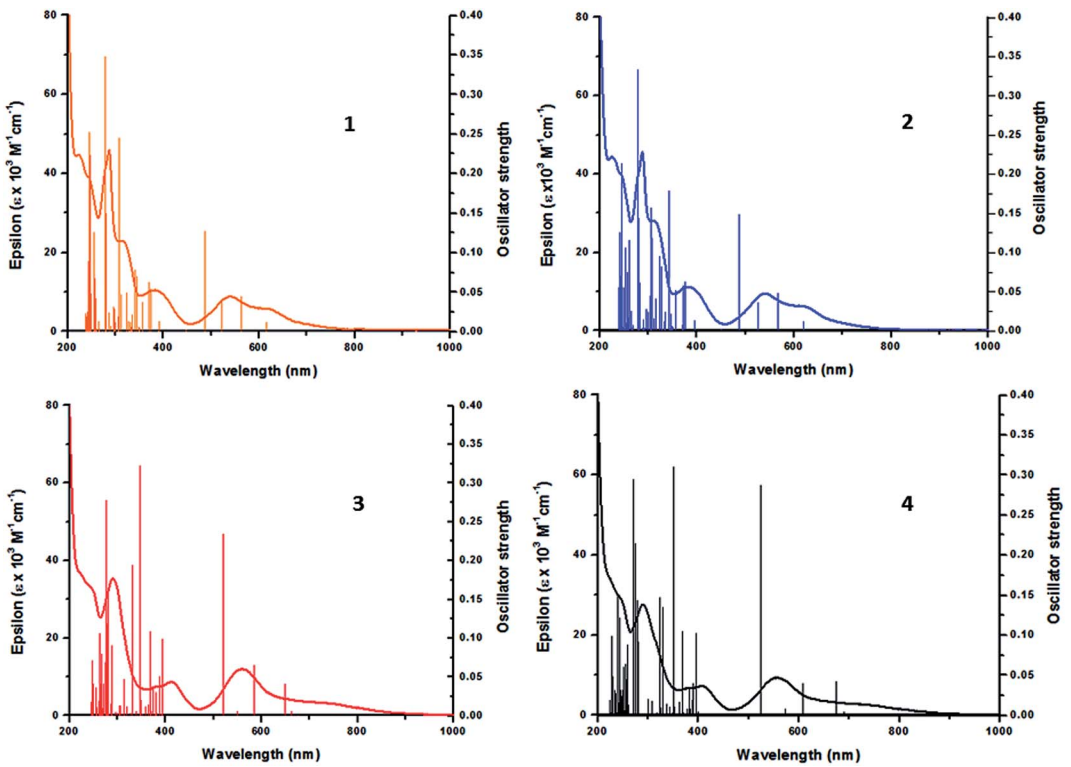

Fig. 9 Overlay of experimental absorption spectra of the complexes **1** (orange), **2** (blue), **3** (red) and **4** (black) in acetonitrile with their predicted transitions and oscillator strength, calculated by TD-DFT.

aforesaid destabilization of the metal-based orbitals (HOMO) by the strongly σ-donating **L1**. The LUMO being triazine-based is now even lower in energy than in **1** or **2**, which results in a smaller HOMO–LUMO gap. In addition to these bands, both **3** and **4** absorb around 415 nm, which may be a transition similar to that found in case of **1** and **2** at 380 nm as supported by TD-DFT calculations of complexes **3** and **4** (see Tables S8 and S10 in ESI†). A red-shift in these bands occurs in going from terpyridine to 2,4-dipyrid-2′-yl-triazine complexes, which may be indicative of its nature as a second MLCT transition, suggesting that the ligand-based π* orbitals are now so low in energy that a transition from HOMO to LUMO+1 is also lowered in energy as compared to tpy–Ru–tpy type complexes.

The luminescence properties of all of the complexes were studied in dry, degassed acetonitrile at room temperature. The corrected emission spectra maxima (λ_{max}) along with lifetime (τ), quantum yield (Φ), and excited-state radiative (k_r) and non-radiative (k_{nr}) decay values are reported in Table 3, while representative emission spectra are shown in Fig. 10. Complexes **1** and **2** exhibit room temperature luminescence in degassed acetonitrile at around 900 nm and these emissions are not quenched in air-equilibrated acetonitrile solutions. As expected, with increased donation the emission wavelength is red-shifted upon introduction of **L1** in place of a terpyridine ligand in $[Ru(Ph\text{-}tpy)_2]^{2+}$ and $[Ru(p\text{-}Tolyl\text{-}tpy)_2]^{2+}$, whereas the emission maxima for the latter two are observed at 715 and 640 nm, respectively. Complexes **3** and **4** are non-luminescent at room temperature, while they were found to be very weakly luminescent at 77 K in rigid butyronitrile matrix (Fig. S7 in ESI†). For complexes **1** and **2**, luminescence energy and the blue-shift of the emission on moving from room temperature fluid solution to 77 K rigid matrix, may indicate that luminescence originates from the (formally) triplet MLCT state involving substituted tpy ligands, as expected. The red-shift of the Ru-to-substituted-tpy/dpt CT emission for all of the studied

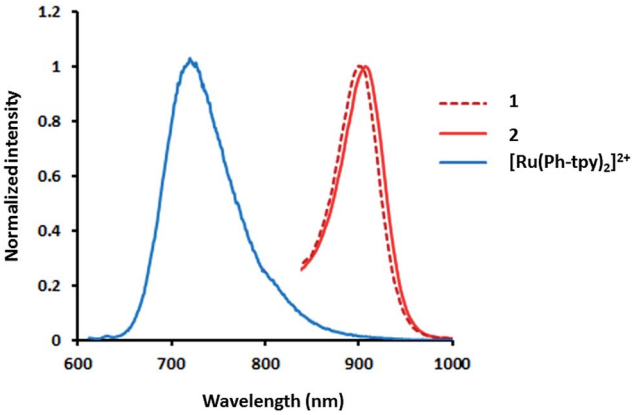

Fig. 10 Normalized emission spectra of complexes **1** and **2** and benchmark complex $[Ru(Ph\text{-}tpy)_2]^{2+}$ in dry, degassed acetonitrile at room temperature.

complexes in comparison to $[Ru(ttpy)_2]^{2+}$ is due to the narrower HOMO–LUMO energy gaps calculated for $[\mathbf{1}]^{2+}$ (2.91 eV), $[\mathbf{2}]^{2+}$ (2.89 eV), $[\mathbf{3}]^{2+}$ (2.59 eV) and $[\mathbf{4}]^{2+}$ (2.52 eV) in comparison to that of $[Ru(tpy)_2]^{2+}$ (3.58 eV),[62] thereby confirming the agreement among redox, TD-DFT, absorption and emission data. Both complexes **1** and **2** exhibit bi-exponential decay for their excited-state lifetimes at room temperature, with a secondary common component of ~8 ns, upon excitation at different ^{1}MLCT maxima even though the experiments were performed with their analytically pure forms. The secondary component may involve a small contribution of ligand-to-ligand CT emission.

The details of the emission behavior can better be understood by recalling the effect of the nonradiative decay rate constant (k_{nr}), which is an added sum of two contributing factors, k^0_{nr} and k'_{nr}. The former is related to the direct deactivation from ^{3}MLCT to the ground-state, whereas the latter is related to the thermally activated process that takes into

Table 3 Spectroscopic and photophysical data in deaerated CH_3CN solutions

	Absorption	Emission @ 298 K*					Emission @ 77 K
Compound	λ_{max}, nm ($\varepsilon \times 10^3$, M^{-1} cm^{-1})	λ_{max} (nm)	τ (ns)	$10^{-4}\Phi$	$10^4 k_r$ (s^{-1})	$10^6 k_{nr}$ (s^{-1})	λ_{max} (nm)
1	541 (5.0)	900	129 (84%), 8 (16%)	10	0.77	7.74	840
	622 (3.3)						
2	538 (9.4)	900	89 (94%), 8 (6%)	10	2.25	11.21	840
	620 (6.2)						
3	560 (11.8)	—	—	—	—	—	935
	740 (3.8)						
4	558 (9.3)	—	—	—	—	—	965
	740 (3.0)						
$[Ru(tpy)_2]^{2+}$	474 (10.4)[a]	629[a]	0.25[b]	≤0.05[a]	2.0	3999.9	598
$[Ru(p\text{-}Tolyl\text{-}tpy)_2]^{2+}$	490 (28.0)[c]	640	0.95	0.32	3.36	1052.6	628[d]
$[Ru(Ph\text{-}tpy)_2]^{2+}$	488 (26.2)[a]	715[a]	1.0[a]	0.40[a]	4.0	999.9	629
$[Ru(tpy)(N\text{^}C\text{^}N)]^+$	499 (14.4)[e]	781[e]	—[f]	0.09[e]	—[f]	—[f]	—[f]
$[Ru(tpy)(Br\text{-}Ph\text{-}dpt)]^{2+}$	476 (21.7)[g]	739[g]	12[g]	1.2[g]	1.0	83.3	693

[a] From ref. 16*a* (using $Ru(bpy)_3(PF_6)_2$ ($\Phi = 0.028$) as standard). [b] From ref. 16*b*. [c] From ref. 16*d*. [d] From ref. 16*d* at 90 K. [e] From ref. 56 (using $Ru(bpy)_3(PF_6)_2$ ($\Phi = 0.062$) as standard). [f] No data available. [g] From ref. 54 (using $[\{(bpy)_2Ru(\mu\text{-}2,3\text{-}dpp)\}_3Ru]^{8+}$ ($\Phi = 0.005$) (2,3-dpp = 2,3-bis(2′-pyridyl)-pyrazine) as standard). * The values of k_r and k_{nr} were calculated using equations $\Phi_{em} = k_r\tau$ and $\tau = (k_r + k_{nr})^{-1}$ as found in ref. 55*d*.

account a surface crossing from the lowest-lying ^{3}MLCT state to a closely lying metal-centered (^{3}MC) level (*i.e.*, the so-called TAIC process in Fig. 1). In general, for Ru(II)-polypyridyl complexes with tridentate ligands the higher values of k_{nr} (Table 3) at 298 K are predominantly contributed by k'_{nr}. This fact is a consequence of lower ligand-field strength experienced by the metal center as compared to that in Ru(II) complexes with bidentate polypyridyl ligands, due to larger deviation from octahedral geometry. The lower values of k_{nr} in complexes **1** and **2**, compared to that of the benchmark complexes, clearly indicates enhanced ^{3}MLCT–^{3}MC energy gap, thus allowing complexes **1** and **2** to exhibit much longer r.t. excited-state lifetime. The non-luminescent nature of complexes **3** and **4** may be explained by enhanced k^0_{nr}, assuming the energy of the ^{3}MC state remaining roughly constant among complexes **1–4**, due to the presence of equal number of donating **hpp** units throughout the series (indeed, the MC level is expected to slightly decrease on passing from **1** and **2** to **3** and **4**). The stabilization of the ^{1}MLCT and consequently the ^{3}MLCT state is achieved by introduction of a better π-accepting triazine core in dpt unit in place of the central pyridine ring in a tpy unit, thereby lowering the energy of metal-based HOMO (Fig. 7). This fact is supported by a red-shift of ^{1}MLCT absorption and ^{3}MLCT emission maxima of complexes **3** and **4** compared to that of **1** and **2** at 77 K, respectively. The increased stabilization of ^{3}MLCT states of complexes **3** and **4** in turn facilitates a direct deactivation to the ground-state, thus rendering them non-luminescent at r.t. However at low temperature the rate of this deactivation is decreased. The effect of dipolar interactions of the heteroatom lone-pair of the dpt core in complexes **3** and **4** with the solvent in quenching the r.t. luminescence may not be excluded either.

Conclusions

In conclusion, we synthesized a N_{amine}-substituted 2,6-diguanidyl-pyridine tridentate ligand, **L1**, that can coordinate to a ruthenium(II) center forming two six-membered chelate rings, and prepared four heteroleptic Ru(II) complexes (**1–4**) using **L1** in connection with four different tridentate ligands. From the Ru(III/II) oxidation potentials of the new complexes, it is found that ligand **L1** has strong donating ability as compared to common polypyridyl tridentate ligands. In particular, the redox behavior of **1–4** suggest that **L1** has similar electron donating capacity as the cyclometallating ligand 1,3-di(2-pyridyl)benzene (N^C^N). As a result of strong donation from ligand **L1**, complexes **1–4** have ^{1}MLCT absorption bands in the visible region at significantly lower energy as compared to $[Ru(tpy)_2]^{2+}$. The ^{1}MLCT absorption maxima of complexes **3** and **4** trail to far-red region of the electromagnetic spectrum. Complexes **1–4** emit at 77 K from a Ru^{II}-to-tridentate-ligand ^{3}MLCT state in the near-infrared region; and these emissions are among the lowest energy ^{3}MLCT luminescence considering mononuclear ruthenium complexes that are octahedrally coordinated by six nitrogen atoms. Complexes **1** and **2** also exhibit room temperature excited-state lifetimes (τ) of 129 ns and 89 ns, with associated quantum yield (Φ) of 0.001. Such emission lifetimes and quantum yields are quite long and large in comparison with those reported by other Ru(II) compounds exhibiting emission at similar energies, and are considered to be due to a very large MLCT-MC energy gap. Thus, the excellent electrochemical and photophysical properties of these complexes, in particular their somewhat unusual long-lived and relatively intense emission in the NIR region, may render them useful for vectorial electron and energy transfer processes in solution or at semiconductor interfaces and also in biological applications as luminescent sensors in cell-imaging systems.

Experimental section

Syntheses of the compounds

Ligand **L1** and complex **1** were synthesized using a literature procedure.[41d] The NMR and mass spectrometric data of these compounds are consistent with the literature values and the elemental analyses of these two compounds were satisfactory. For the syntheses of **L2** and complexes **2–4**, materials, methods and instruments used see ESI.†

Computational details

All calculations were performed with the Gaussian03 (ref. 63) employing the DFT method, the Becke three-parameter hybrid functional,[64] and Lee–Yang–Parr's gradient-corrected correlation functional (B3LYP).[65] Singlet ground state geometry optimizations for $[\mathbf{1}]^{2+}$, $[\mathbf{2}]^{2+}$, $[\mathbf{3}]^{2+}$ and $[\mathbf{4}]^{2+}$ were carried out at the (R)B3LYP level in the gas phase, using their respective crystallographic structures as starting points. All elements except Ru were assigned the 6-31G(d,f) basis set.[66] The LANL2DZ basis set[67] with an effective core potential and one additional f-type polarization was employed for the Ru atom. Vertical electronic excitations based on (R)B3LYP-optimized geometries were computed for $[\mathbf{1}]^{2+}$, $[\mathbf{2}]^{2+}$, $[\mathbf{3}]^{2+}$ and $[\mathbf{4}]^{2+}$ using the TD-DFT formalism[68] in acetonitrile using conductor-like polarizable continuum model (CPCM).[69] Vibrational frequency calculations were performed to ensure that the optimized geometries represent the local minima and there are only positive eigenvalues. The electronic distribution and localization of the singlet excited states were visualized using the electron density difference maps (ED-DMs).[70] *Gausssum 2.2* was employed to draw absorption spectra (simulated with Gaussian distribution with a full-width at half maximum (fwhm) set to 3000 cm^{-1}) and to calculate the fractional contributions of various groups to each molecular orbital. All calculated structures were visualized with ChemCraft.[71]

Acknowledgements

AKP and GSH thank Natural Sciences and Engineering Research Council of Canada (NSERC) and Centre for Self-Assembled Chemical Structure (CSACS) and the Université de Montréal for financial support. SC thanks MIUR (FIRB: Nanosolar and PRIN: Hi-Phuture projects) for funding.

Notes and references

1 (*a*) A. Hagfeldt and M. Graetzel, *Chem. Rev.*, 1995, **95**, 49; (*b*) L. C. Sun, L. Hammarström, B. Åkermark and S. Styring, *Chem. Soc. Rev.*, 2001, **30**, 36; (*c*) J. G. Vos and J. M. Kelly, *Dalton Trans.*, 2006, 4869; (*d*) S. Arlo and G. J. Meyer, *Chem. Soc. Rev.*, 2009, **38**, 115 and references therein; (*e*) J. J. Concepcion, J. W. Jurss, M. K. Brennaman, P. G. Hoertz, A. O. T. Patrocinio, N. Y. M. Iha, J. L. Templeton and T. J. Meyer, *Acc. Chem. Res.*, 2009, **42**, 1954; (*f*) Z. F. Chen, J. J. Concepcion, X. Q. Hu, W. T. Yang, P. G. Hoertz and T. J. Meyer, *Proc. Natl. Acad. Sci. U. S. A.*, 2010, **107**, 7225; (*g*) F. Puntoriero, A. Sartorel, M. Orlandi, G. La Ganga, S. Serroni, M. Bonchio, F. Scandola and S. Campagna, *Coord. Chem. Rev.*, 2011, **255**, 2594 and references therein; (*h*) P. G. Bomben, K. C. D. Robson, B. D. Koivisto and C. P. Berlinguette, *Coord. Chem. Rev.*, 2012, **256**, 1438 and references cited therein; (*i*) J. R. Swierk and T. E. Mallouk, *Chem. Soc. Rev.*, 2013, **42**, 2357; (*j*) V. Balzani, G. Bergamini, S. Campagna and F. Puntoriero, *Top. Curr. Chem.*, 2007, **280**, 1.

2 M. R. Gill, J. Garcia-Lara, S. J. Foster, C. Smythe, G. Battaglia and J. A. Thomas, *Nat. Chem.*, 2009, **1**, 662.

3 (*a*) H. J. Bolink, L. Cappelli, E. Coronado and P. Gavina, *Inorg. Chem.*, 2005, **44**, 5966; (*b*) H. J. Bolink, L. Cappelli, E. Coronado, M. Graetzel and M. K. Nazeeruddin, *J. Am. Chem. Soc.*, 2006, **128**, 46.

4 (*a*) T. J. Meyer, *Pure Appl. Chem.*, 1986, **58**, 1193; (*b*) D. W. Thompson, A. Ito and T. J. Meyer, *Pure Appl. Chem.*, 2013, **85**, 1257.

5 (*a*) A. Juris, V. Balzani, F. Barigelletti, S. Campagna, P. Belser and A. von Zelewsky, *Coord. Chem. Rev.*, 1988, **84**, 85; (*b*) V. Balzani, A. Juris, M. Venturi, S. Campagna and S. Serroni, *Chem. Rev.*, 1996, **96**, 759.

6 J.-P. Sauvage, J. P. Collin, J. C. Chambron, S. Guillerez, C. Coudret, V. Balzani, F. Barigelletti, L. De Cola and L. Flamigni, *Chem. Rev.*, 1994, **94**, 993.

7 E. Baranoff, J. P. Collin, L. Flamigni and J.-P. Sauvage, *Chem. Soc. Rev.*, 2004, **33**, 147.

8 S. Baitalik, X. Wang and R. H. Schmehl, *J. Am. Chem. Soc.*, 2004, **126**, 16304.

9 (*a*) C. Bhaumik, D. Saha, S. Das and S. Baitalik, *Inorg. Chem.*, 2011, **50**, 12586; (*b*) J. Fortage, G. Dupeyre, F. Tuyèras, V. Marvaud, P. Ochsenbein, I. Ciofini, M. Hromadová, L. Pospísil, A. Arrigo, E. Trovato, F. Puntoriero, P. P. Lainé and S. Campagna, *Inorg. Chem.*, 2013, **52**, 11944.

10 M. Jäger, A. Smeigh, F. Lombeck, H. Görls, J.-P. Collin, J.-P. Sauvage, L. Hammarström and O. Johansson, *Inorg. Chem.*, 2010, **49**, 374.

11 E. C. Constable, *Chem. Soc. Rev.*, 2004, **33**, 246.

12 H. Hofmeier and U. S. Schubert, *Chem. Soc. Rev.*, 2004, **33**, 373.

13 (*a*) E. A. Medlycott and G. S. Hanan, *Coord. Chem. Rev.*, 2006, **250**, 1763; (*b*) E. A. Medlycott and G. S. Hanan, *Chem. Soc. Rev.*, 2005, **34**, 133; (*c*) A. K. Pal and G. S. Hanan, *Chem. Soc. Rev.*, 2014, **43**, 6184–6197.

14 X.-Y. Wang, A. Del Guerzo and R. H. Schmehl, *J. Photochem. Photobiol., C*, 2004, **5**, 55.

15 A. I. Baba, J. R. Shaw, J. A. Simon, R. P. Thummel and R. H. Schmehl, *Coord. Chem. Rev.*, 1998, **171**, 43.

16 (*a*) M. Maestri, N. Armaroli, V. Balzani, E. C. Constable and A. Thompson, *Inorg. Chem.*, 1995, **34**, 2759; (*b*) M. Beley, J. P. Collin, J. P. Sauvage, H. Sugihara, F. Heisel and A. Miehe, *J. Chem. Soc., Dalton Trans.*, 1991, 315; (*c*) G. J. E. Davidson, S. J. Loeb, P. Passaniti, S. Silvi and A. Credi, *Chem.–Eur. J.*, 2006, **12**, 3233; (*d*) J. P. Collin, S. Guillerez, J. P. Sauvage, F. Barigelletti, L. De Cola, L. Flamigni and V. Balzani, *Inorg. Chem.*, 1991, **30**, 4230.

17 (*a*) J. R. Winkler, T. Netzel, C. Creutz and N. Sutin, *J. Am. Chem. Soc.*, 1987, **109**, 2381; (*b*) B. O'Regan and M. Gräetzel, *Nature*, 1991, **353**, 737.

18 J. M. Calvert, J. V. Caspar, R. A. Binstead, T. D. Westmoreland and T. J. Meyer, *J. Am. Chem. Soc.*, 1982, **104**, 6620.

19 (*a*) J. H. Wang, Y. Q. Fang, G. S. Hanan, F. Loiseau and S. Campagna, *Inorg. Chem.*, 2005, **44**, 5; (*b*) E. C. Constable, A. M. W. Cargill Thompson, N. Armaroli, V. Balzani and M. Maestri, *Polyhedron*, 1992, **11**, 2707.

20 M. I. J. Polson, F. Loiseau, S. Campagna and G. S. Hanan, *Chem. Commun.*, 2006, 1301.

21 Y.-Q. Fang, N. J. Taylor, F. Laverdiere, G. S. Hanan, F. Loiseau, F. Nastasi, S. Campagna, H. Nierengarten, E. Leize-Wagner and A. Van Dorsselaer, *Inorg. Chem.*, 2007, **46**, 2854.

22 Y.-Q. Fang, N. J. Taylor, G. S. Hanan, F. Loiseau, R. Passalacqua, S. Campagna, H. Nierengarten and A. Van Dorsselaer, *J. Am. Chem. Soc.*, 2002, **124**, 7912.

23 S. Encinas, L. Flamigni, F. Barigelletti, E. C. Constable, C. E. Housecroft, E. R. Schofield, E. Figgemeier, D. Fenske, M. Neuburger, J. G. Vos and M. Zehnder, *Chem.–Eur. J.*, 2002, **8**, 137.

24 (*a*) M. Hissler, A. El-ghayoury, A. Harriman and R. Ziessel, *Angew. Chem., Int. Ed.*, 1998, **37**, 1717; (*b*) A. Barbieri, B. Ventura and R. Ziessel, *Coord. Chem. Rev.*, 2012, **256**, 1732 and references cited therein; (*c*) P. Manca, M. I. Pilo, G. Sanna, A. Zucca, G. Bergamini and P. Ceroni, *Chem. Commun.*, 2011, **47**, 3413.

25 R. Passalacqua, F. Loiseau, S. Campagna, Y.-Q. Fang and G. S. Hanan, *Angew. Chem., Int. Ed.*, 2003, **42**, 1608.

26 J. Wang, G. S. Hanan, F. Loiseau and S. Campagna, *Chem. Commun.*, 2004, 2068.

27 J. Wang, Y.-Q. Fang, L. Bourget-Merle, M. I. J. Polson, G. S. Hanan, A. Juris, F. Loiseau and S. Campagna, *Chem.–Eur. J.*, 2006, **12**, 8539.

28 (*a*) N. D. McClenaghan, Y. Leydet, B. Maubert, M. T. Indelli and S. Campagna, *Coord. Chem. Rev.*, 2005, **249**, 1336; (*b*) G. Ragazzon, P. Verwilst, S. A. Denisov, A. Credi, G. Jonusauskas and N. D. McClenaghan, *Chem. Commun.*, 2013, **49**, 9110.

29 M. Beley, S. Chodorowski, J.-P. Collin, J.-P. Sauvage, L. Flamigni and F. Barigelletti, *Inorg. Chem.*, 1994, **33**, 2543.

30 M. T. Indelli, C. A. Bignozzi, F. Scandola and J.-P. Collin, *Inorg. Chem.*, 1998, **37**, 6084.

31 M. Duati, S. Fanni and J. G. Vos, *Inorg. Chem. Commun.*, 2000, **3**, 68.
32 M. Duati, S. Tasca, F. C. Lynch, H. Bohlen, J. G. Vos, S. Stagni and M. D. Ward, *Inorg. Chem.*, 2003, **42**, 8377.
33 S. U. Son, K. H. Park, Y.-S. Lee, B. Y. Kim, C. H. Choi, M. S. Lah, Y. H. Jang, D.-J. Jang and Y. K. Chung, *Inorg. Chem.*, 2004, **43**, 6896.
34 J. P. Collin, M. Beley, J. P. Sauvage and F. Barigelletti, *Inorg. Chim. Acta*, 1991, **186**, 91.
35 (*a*) S. H. Wadman, J. M. Kroon, K. Bakker, R. W. A. Havenith, G. P. M. van Klink and G. van Koten, *Organometallics*, 2010, **29**, 1569; (*b*) D. G. Brown, N. Sanguantrakun, B. Schulze, U. S. Schubert and C. P. Berlinguette, *J. Am. Chem. Soc.*, 2012, **134**, 12354; (*c*) F. Barigelletti, B. Ventura, J.-P. Collin, R. Kayhanian, P. Gaviña and J.-P. Sauvage, *Eur. J. Inorg. Chem.*, 2000, **1**, 113.
36 (*a*) M. Abrahamsson, H. Wolpher, O. Johansson, J. Larsson, M. Kritikos, L. Eriksson, P.-O. Norrby, J. Bergquist, L. Sun, B. Åkermark and L. Hammarström, *Inorg. Chem.*, 2005, **44**, 3215; (*b*) M. Abrahamsson, M. J. Lundqvist, H. Wolpher, O. Johansson, L. Eriksson, J. R. T. Bergquist, H.-C. Becker, L. Hammarström, P. O. Norrby, B. Åkermark and P. Persson, *Inorg. Chem.*, 2008, **47**, 3540.
37 (*a*) F. Schramm, V. Meded, H. Fliegl, K. Fink, O. Fuhr, Z. Qu, W. Klopper, S. Finn, T. E. Keyes and M. Ruben, *Inorg. Chem.*, 2009, **48**, 5677; (*b*) A. Breivogel, M. Meister, C. Fçrster, F. Laquai and K. Heinze, *Chem.–Eur. J.*, 2013, **19**, 13745 and references cited therein.
38 (*a*) J.-L. Chen, Y. Chi and K. Chen, *Inorg. Chem.*, 2010, **49**, 823; (*b*) G. Dyker and O. Muth, *Eur. J. Org. Chem.*, 2004, 4319.
39 X.-D. Chen and T. C. W. Mak, *Inorg. Chim. Acta*, 2005, **358**, 1107.
40 (*a*) M. Abrahamsson, M. Jäger, T. Österman, L. Eriksson, P. Persson, H.-C. Becker, O. Johansson and L. Hammarström, *J. Am. Chem. Soc.*, 2006, **128**, 12616; (*b*) M. Jäger, R. J. Kumar, H. Görls, J. Bergquist and O. Johansson, *Inorg. Chem.*, 2009, **48**, 3228.
41 (*a*) S. Nag, J. G. Ferreira, L. Chenneberg, P. D. Ducharme, G. S. Hanan, G. La Ganga, S. Serroni and S. Campagna, *Inorg. Chem.*, 2011, **50**, 7; (*b*) A. K. Pal, S. Nag, J. G Ferreira, V. Brochery, G. La Ganga, A. Santoro, S. Serroni, S. Campagna and G. S. Hanan, *Inorg. Chem.*, 2014, **53**, 1679; (*c*) A. K. Pal, P. D. Ducharme and G. S. Hanan, *Chem. Commun.*, 2014, **50**, 3303; (*d*) A. K. Pal, N. Zaccheroni, S. Campagna and G. S. Hanan, *Chem. Commun.*, 2014, **50**, 6846–6849; (*e*) A. K. Pal and G. S. Hanan, *Dalton Trans.*, 2014, **43**, 6567; (*f*) A. K. Pal, B. Laramée-Milette and G. S. Hanan, *Inorg. Chim. Acta*, 2014, **418**, 15; (*g*) A. K. Pal, B. Laramée-Milette and G. S. Hanan, *RSC Adv.*, 2014, **4**, 21262.
42 M. P. Coles, *Chem. Commun.*, 2009, 3659.
43 U. Wild, P. Roquette, E. Kaifer, J. Mautz, O. Huebner, H. Wadepohl and H.-J. Himmel, *Eur. J. Inorg. Chem.*, 2008, 1248.
44 M. Abrahamsson, M. Jäger, R. J. Kumar, T. Österman, P. Persson, H.-C. Becker, O. Johansson and L. Hammarström, *J. Am. Chem. Soc.*, 2008, **130**, 15533.
45 R. J. Kumar, S. Karlsson, D. Streich, A. Rolandini Jensen, M. Jäger, H.-C. Becker, J. Bergquist, O. Johansson and L. Hammarström, *Chem.–Eur. J.*, 2010, **16**, 2830.
46 J. P. Wolfe and S. L. Buchwald, *J. Org. Chem.*, 2000, **65**, 1144.
47 S. H. Oakley, M. P. Coles and P. B. Hitchcock, *Inorg. Chem.*, 2004, **43**, 7564.
48 (*a*) M. I. J. Polson, E. A. Medlycott, G. S. Hanan, L. Mikelsons, N. J. Taylor, M. Watanabe, Y. Tanaka, F. Loiseau, R. Passalacqua and S. Campagna, *Chem.–Eur. J.*, 2004, **10**, 3640; (*b*) E. A. Medlycott, K. A. Udachin and G. S. Hanan, *Dalton Trans.*, 2007, 430.
49 For a general introduction to the synthesis of bisterpyridyl ruthenium(II) complexes, see: (*a*) U. S. Schubert, H. Hofmeier and G. R. Newkome, *Modern Terpyridine Chemistry*, WILEY-VCH, Weinheim, 2006; (*b*) H. Hofmeier and U. S. Schubert, *Chem. Soc. Rev.*, 2004, **33**, 373.
50 J. McMurtriea and I. Dance, *CrystEngComm*, 2009, **11**, 1141.
51 J. E. Beves, P. Chwalisz, E. C. Constable, C. E. Housecroft, M. Neuburger, S. Schaffner and J. A. Zampese, *Inorg. Chem. Commun.*, 2008, **11**, 1009.
52 S. Pyo, E. P. Cordero, S. G. Bott and L. Echegoyen, *Inorg. Chem.*, 1999, **38**, 3337.
53 (*a*) B. De Groot, G. S. Hanan and S. J. Loeb, *Inorg. Chem.*, 1991, **30**, 4644; (*b*) G. R. Giesbrecht, G. S. Hanan, J. E. Kickham and S. J. Loeb, *Inorg. Chem.*, 1992, **31**, 3286.
54 E. A. Medlycott, G. S. Hanan, F. Loiseau and S. Campagna, *Chem.–Eur. J.*, 2007, **13**, 2837.
55 (*a*) A. Harriman, A. Mayeux, A. D. Nicola and R. Ziessel, *Phys. Chem. Chem. Phys.*, 2002, **4**, 2229; (*b*) E. C. Constable, A. M. W. C. Thompson, D. A. Tocher and M. A. M. Daniels, *New J. Chem.*, 1992, **16**, 855; (*c*) J. T. Hewitt, P. J. Vallett and N. H. Damrauer, *J. Phys. Chem. A*, 2012, **116**, 11536; (*d*) K. R. Barqawi, Z. Murtaza and T. J. Meyer, *J. Phys. Chem.*, 1991, **95**, 47.
56 S. H. Wadman, M. Lutz, D. M. Tooke, A. L. Spek, F. Hartl, R. W. A. Havenith, G. P. M. van Klink and G. van Koten, *Inorg. Chem.*, 2009, **48**, 1887.
57 P. G. Bomben, K. C. D. Robson, P. A. Sedach and C. P. Berlinguette, *Inorg. Chem.*, 2009, **48**, 9631.
58 U. Siemeling, J. V. der Bruggen, U. Vorfeld, B. Neumann, A. Stammler, H.-G. Stammler, A. Brockhinke, R. Plessow, P. Zanello, F. Laschi, F. F. de Biani, M. Fontani, S. Steenken, M. Stapper and G. Gurzadyan, *Chem.–Eur. J.*, 2003, **9**, 2819.
59 I. Hanazaki and S. Nagakura, *Inorg. Chem.*, 1969, **8**, 648.
60 G. M. Bryant, J. E. Fergusson and H. K. J. Powell, *Aust. J. Chem.*, 1971, **24**, 257.
61 N. Aydin and C. W. Schlaepfer, *Polyhedron*, 2001, **20**, 37.
62 H. J. Bolink, E. Coronado, R. D. Costa, P. Gaviña, E. Ortí and S. Tatay, *Inorg. Chem.*, 2009, **48**, 3907.
63 M. J. Frisch, G. W. Trucks, H. B. Schlegel, G. E. Scuseria, M. A. Robb, J. R. Cheeseman, J. A. Montgomery, T. J. Vreven, K. N. Kudin, J. C. Burant, J. M. S. Millam, J. Tomasi, V. Barone, B. Mennucci, M. Cossi, G. Scalmani, N. Rega, G. A. Petersson, H. Nakatsuji, M. Hada, M. Ehara, K. Toyota, R. Fukuda, J. Hasegawa, M. Ishida, T. Nakajima, Y. Honda, O. Kitao, H. Nakai, M. Klene, X. Li, J. E. Knox,

H. P. Hratchian, J. B. Cross, C. Adamo, J. Jaramillo, R. Gomperts, R. E. Startmann, O. Yazyev, A. J. Austin, R. Cammi, C. Pomelli, J. W. Ochterski, P. Y. Ayala, K. Morokuma, G. A. Voth, P. Salvador, J. J. Dannenberg, V. G. Zakrzewski, J. M. Dapprich, A. D. Daniels, M. C. Strain, O. Farkas, D. K. Malick, A. D. Rabuck, K. Raghavachari, J. B. Foresman, J. V. Ortiz, Q. Cui, A. G. Baboul, S. Cliffors, J. B. Cioslowski, G. Liu, A. Liashenko, I. Piskorz, I. L. M. R. Komaromi, D. J. Fox, T. Keith, M. A. Al-Laham, C. Y. Peng, A. Manayakkara, M. Challacombe, P. M. W. Gill, B. G. Johnson, W. Chen, M. W. Wong, C. Gonzalez and J. A. Pople, *Gaussian 2003, Revision C.02*, Gaussian Inc., Pittsburgh PA, 2003.

64 A. D. Becke, *J. Chem. Phys.*, 1993, **98**, 5648.

65 C. Lee, W. Yang and R. G. Parr, *Phys. Rev. B: Condens. Matter*, 1988, **37**, 785.

66 A. D. McLean and G. S. Chandler, *J. Chem. Phys.*, 1980, **72**, 5639.

67 P. J. Hay and W. R. Wadt, *J. Chem. Phys.*, 1985, **82**, 270.

68 (*a*) M. E. Casida, C. Jamorski, K. C. Casida and D. R. Salahub, *J. Chem. Phys.*, 1998, **108**, 4439; (*b*) R. E. Stratmann, G. E. Scuseria and M. J. Frisch, *J. Chem. Phys.*, 1998, **109**, 8218.

69 (*a*) M. Cossi, N. Rega, G. Scalmani and V. Barone, *J. Comput. Chem.*, 2003, **24**, 669; (*b*) M. Cossi and V. Barone, *J. Chem. Phys.*, 2001, **115**, 4708; (*c*) V. Barone and M. Cossi, *J. Phys. Chem. A*, 1998, **102**, 1995.

70 W. R. Browne, N. M. O'Boyle, J. J. McGarvey and J. G. Vos, *Chem. Soc. Rev.*, 2005, **34**, 641.

71 D. A. Zhurko and G. A. Zhurko, *ChemCraft 1.5*, Plimus, San Diego, CA, http://www.chemcraftprog.com.